Astron. Astrophys. 208, 189–197 (1989)

ASTRONOMY AND ASTROPHYSICS

# Magnetic fields in late-type dwarfs: Preliminary results from a multiline approach ⋆

**G. Mathys** [1] **and S. K. Solanki** [2]

[1] Observatoire de Genève, chemin des Maillettes, 51, CH-1290 Sauverny, Switzerland
[2] Department of Mathematical Sciences, University of St. Andrews, St. Andrews, KY16 9SS, Scotland

Received March 30, accepted July 4, 1988

**Summary.** Preliminary results of a multiline approach to the diagnosis of magnetic fields in late-type dwarfs are presented. The spectra of four stars observed with the Coudé Echelle Spectrometer of the European Southern Observatory are analysed using the Stenflo-Lindegren technique, which permits empirical relations to be obtained between various parameters characterizing a statistical sample of observed line profiles and the atomic quantities pertaining to the corresponding transitions. These empirical relations are first tested on solar and stellar data and then interpreted with the help of a simple model of the line formation, and constraints on the magnetic field properties (mean strength, filling factor, thermodynamic properties of the magnetic regions compared to the non-magnetic parts of the stellar surface) are derived. In spite of the crudeness of some of the approximations that are made (some unanswered questions will require a more sophisticated treatment), the results are compatible with those previously obtained with other methods. The advantages of the Stenflo-Lindegren technique over these other approaches are sketched out.

**Key words:** stars: late-type – stars: magnetic field

## 1. Introduction

The activity of the sun and stars is caused by magnetic fields and it is basic for our understanding of many phenomena observed in late-type stars (e.g. spots, plages, flares, activity cycles and heating of coronae) to know their magnetic field. Direct determinations of magnetic fields in late-type stars are still few, however, due to the inherent difficulty of such measurements.

In the atmospheres of nondegenerate stars, the magnetic splitting of the spectral lines is most often very small compared to the intrinsic line width (as resulting from the combination of natural width, thermal and microturbulent Doppler broadening, Stark effect, van der Waals interaction, ...) so that the individual Zeeman components are not resolved and the observable manifestation of the magnetic field is a subtle broadening of the line (typically amounting to a few hundreths of an Ångström). On the other hand, due to the different polarization properties of the $\pi$, $\sigma_\pm$ components, the wavelength $\lambda_R$ of the centre of gravity of a spectral line recorded in right circular polarization differs from that ($\lambda_L$) of the same line recorded in left circularly polarized light. For weak absorption lines, the shift $\lambda_R - \lambda_L$ can be shown to be proportional to the component of the magnetic vector along the line of sight, $H_z$ (note that the sign of $H_z$ is important, with $H_z$ being positive for a magnetic vector pointing towards the observer):

$$\lambda_R - \lambda_L = 2k\bar{g}\lambda_0^2 H_z, \quad (1)$$

with $k = 4.67\ 10^{-13}$ Å$^{-1}$ G$^{-1}$, $\bar{g}$ the effective Landé factor of the line and $\lambda_0$ the line centre wavelength in the absence of a magnetic field. For the typical field values observed in nondegenerate stars, the order of magnitude of $\lambda_R - \lambda_L$ is the same as that of the line broadening in unpolarized spectra. Still, since line displacements are much more easily measured than profile changes, especially in moderate $S/N$ spectra, the polarimetric approach has for a long time been the only successful one for the measurement of stellar magnetic fields.

The above discussion pertains to a spectral line emerging from one point of the stellar surface. In actual observations, the lines that are recorded are averages over the whole visible stellar hemisphere. In this case the shift $\lambda_R - \lambda_L$ between the central wavelengths of the right and left circularly polarized profiles is still (for weak lines) expressed by Eq. (1), provided that $H_z$ now represents the line-intensity weighted average over the stellar disk of the line-of-sight component of the magnetic field. If the stellar field has a complex structure, the effects of regions having fields of opposite polarities will cancel out in the averaging process, so that the net polarimetric signal will come close to zero. Observations suggest that such is indeed the case (e.g. Borra et al., 1984). Like on the sun, the magnetic field on other late-type stars is concentrated into bundles of flux with field strengths of the order of a couple of thousand G, surrounded by a practically field-free atmosphere. A large number of such so-called fluxtubes is distributed over the solar or stellar surface, so that at any given time almost equal amounts of flux of both polarities are present on the visible solar or stellar hemisphere. Therefore, for more than thirty years starting with Babcock's (1947) discovery of a magnetic field in 78 Vir, the only nondegenerate stars in which magnetic fields had been firmly detected were Ap or Bp stars, because the magnetic field of these objects has the unique property of having a sufficient large-scale organization to permit its observation through spectropolarimetry. In the beginning of the eighties, a breakthrough occurred with the advent of efficient electronic

*Send offprint requests to:* G. Mathys

⋆ Based on observations collected at the European Southern Observatory, La Silla, Chile

detectors allowing to record line profiles at high spectral resolution with large $S/N$ ratios. Then following the pioneering work of Robinson (1980) and Robinson et al. (1980), studies of line broadening led to the discovery of magnetic fields in a number of stars of spectral types G to M (e.g. Giampapa et al., 1983; Marcy, 1984; Gray, 1984; Gondoin et al., 1985; Saar and Linsky, 1985; Saar et al., 1986; Saar, 1988). Indeed, unlike $\lambda_R - \lambda_L$, Zeeman broadening of spectral lines primarily depends on the modulus of the magnetic field and thus does not cancel out through averaging over the stellar disk. However, line broadening can have a number of non-magnetic causes as well. Robinson's ingenious technique distinguishes between magnetic and non-magnetic broadening by comparing two lines having different effective Landé factors, but which are otherwise similar and, as a result, react similarly to most non-magnetic broadening mechanisms. In what follows, we present preliminary results of a first attempt at diagnosing magnetic fields in late-type dwarfs, using a statistical analysis of a large number of spectral lines. This so-called Stenflo-Lindegren technique has certain advantages over the Robinson technique.

## 2. The observations

The observations were performed with the Coudé Echelle Spectrometer (CES) fed by the Coudé Auxiliary Telescope (CAT) of the European Southern Observatory. The CES was used in its long camera mode; the detector was the RETICON; the achieved spectral resolution was 100000. The main steps of the reduction were as follows: subtraction of the bias and of the dark current, division by the flat-field, normalization to the continuum and wavelength calibration. The dark current was linearly interpolated between the masked pixels at both edges of the RETICON array. This was thought preferable to using a set of independent dark exposures since such exposures do not appear to be reproducible; moreover, there is some indication that the dark current depends to some extent on the magnitude of the observed object. The achieved $S/N$ was in no case lower than 250.

As we intended to apply the Stenflo-Lindegren technique, which, as we describe below, relies on the simultaneous consideration of a large number of spectral line profiles, and as the wavelength range covered in one exposure with the CES is quite short (about 50 Å) and contains only few suitable lines, each star had to be observed consecutively in several different wavelength ranges over the same night. The maximum number of these ranges that could be recorded for a given star was most often dictated by the fairly severe pointing limits of the CAT.

The data upon which the results reported here are based were collected during two runs, in October 1986 and October 1987. Information about the observations is given in Table 1. Columns 1 and 2 contain the star's name and HR number, and Columns 3 and 4 the $V$ magnitude and spectral type. The duration of observation listed in Column 6 refers to the time elapsed between the beginning of the exposure of the first observed wavelength range and the end of the exposure of the last observed wavelength range, and the date in Column 5 corresponds to the middle of that time interval.

## 3. The analysis

As mentioned above, we analysed our data in search of magnetic fields using the Stenflo-Lindegren technique (Stenflo and Lindegren, 1977). The basic idea of this approach, which was first developed to diagnose spatially unresolved magnetic fields on the sun, is to derive empirically the mutual correlations between parameters characterizing the observed line profiles as well as the dependences of these parameters on atomic quantities pertaining to the transition from which the line is formed (for instance, the excitation potential of the lower level of the transition or the effective Landé factor). A regression analysis is performed to quantify the observed dependences. The coefficients are interpreted within the frame of a more or less sophisticated model of the line formation in order to set constraints on the physical conditions prevailing within the stellar atmosphere, in particular the magnetic field. The Stenflo-Lindegren technique has previously been successfully applied to solar spectra (Stenflo and Lindegren, 1977; Solanki and Stenflo, 1984; Brandt and Solanki, 1987) and data from Ap stars (Mathys and Stenflo, 1986).

The parameterization of the line profiles is illustrated in Fig. 1 (we look at profiles normalized to the continuum intensity). $d$ is the depth of the line, expressed as a fraction of the continuum intensity (it thus has values between 0 and 1). A second parameter is the chord length at depth $zd$ above the line bottom; typically we consider $z = 0.3$, 0.5, and 0.7. This chord length is expressed in units of the formal Doppler width $v_D$ of a Gaussian $\exp(-v^2/v_D^2)$ that has the same width at the given level as the observed profile. Finally, the area $S_I$ of the line below the half-depth chord is used to

**Table 1.** Observations of late-type stars with the CES at the CAT

| Name | HR | $V$ | Sp. | Date HJD 2 440 000.+ | Duration (hours) |
|---|---|---|---|---|---|
| $\tau$ Cet | 509 | 3.50 | G8V | 6718.70 | 8.4 |
| $\epsilon$ Eri | 1084 | 3.73 | K2V | 6722.76 | 4.7 |
| 40 Eri A | 1325 | 4.42 | K1V | 6723.75 | 5.8 |
| $\epsilon$ Ind | 8387 | 4.69 | K4-5V | 7189.63 | 5.0 |

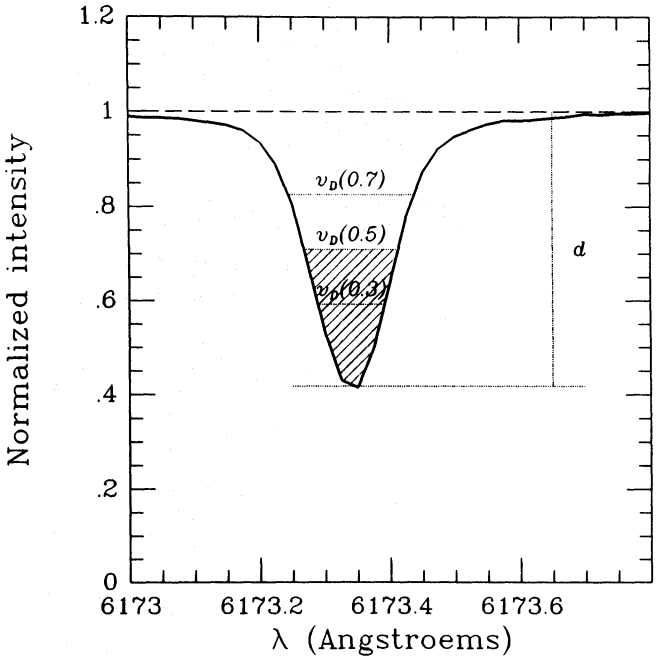


**Fig. 1.** The parameters used to characterize the line profiles are shown on this plot of the line Fe I $\lambda$ 6173.34, as observed in the spectrum of HR 1084. The line-intensity parameter $S_I$ corresponds to the hatched area below the half-depth chord. The definition of the other parameters is evident from the figure (see also text)

characterize the line intensity; it is expressed in Fraunhofers. By using this parameterization we avoid the wings of the line, which are prone to be affected by small blends. For the cases when it may be of advantage to consider the line wings as well, we can easily extend the parameterization.

The parameters introduced above were determined in each star for a sample of (apparently) unblended Fe I lines. The dependences of their chord length $v_D(z)$ on various other parameters were investigated, and it was found that the behaviour of $v_D$ was well represented by an equation of the form (more details are to be found in Sect. 4):

$$v_D(z) = x_0 + x_1 S_I + x_2 S_I^2 + x_3 \chi_e v_0 + x_4 \lambda_0^2/v_0 + x_5 X_m \lambda_0^2/v_0. \quad (2)$$

The coefficients $x_0, \ldots, x_5$ were determined through a multivariate regression analysis. The $x_1$ and $x_2$ terms contain the main dependences of $v_D$ on $S_I$. The $x_3$ term includes the dependence on $\chi_e$, the excitation potential of the lower level of the transition. The dependence of $v_D$ on $\chi_e$ is mainly due to the much larger van der Waals damping constants of high excitation lines compared to otherwise similar low excitation lines. The $\chi_e$ term is multiplied by $v_0$, an approximation to $v_D$ (see below), since the dependence on excitation potential is observed to increase with increasing line width. This is due to the fact that the influence of the damping constant on the line profile, in particular its half-width, increases dramatically with saturation. The $x_4$ term represents that part of the wavelength dependence of $v_D$ which is unrelated to the magnetic field. Following Stenflo and Lindegren (1977) we have given it a form similar to the magnetic broadening of $x_5$ term. $X_m$ characterizes the sensitivity of the line width to a magnetic field:

$$X_m = (\bar{g}^2 + X_\sigma)\frac{1+\cos^2\gamma}{2} + X_\pi \frac{\sin^2\gamma}{2}. \quad (3)$$

$\bar{g}$ is, as indicated before, the effective Landé factor of the line, which accounts for the mean shift of the $\sigma$ components from the line centre $\lambda_0$, and $X_\sigma$ and $X_\pi$ are the second order moments about their centre of gravity of the $\sigma_+$ and $\pi$ components respectively, which account for the spread of these components about their average wavelength. $\gamma$ is the angle between the magnetic field and the line of sight. Values of $\chi_e$ have been listed for unblended Fe I lines by Stenflo and Lindegren (1977). Whenever possible, the values of $\bar{g}$, $X_\sigma$, and $X_\pi$ have been calculated as described by Landi Degl' Innocenti (1980) or Mathys and Stenflo (1987) from the experimental value of the Landé factors of the levels involved in the transition (Sugar and Corliss, 1985). When laboratory $g$ values were not available, $LS$-coupling values were used instead. Finally, $v_0$ is an approximate value of the chord length at the given depth, obtained in the following way. As illustrated in Fig. 2a, where $v_D$ (0.5) is plotted vs. $S_I$, the most obvious dependence of the chord length is on the line intensity. This dependence is satisfactorily represented by a second-degree polynomial:

$$v_D(z) = y_0 + y_1 S_I + y_2 S_I^2. \quad (4)$$

The fitted value $v_0$ of the chord length is computed from the line intensity $S_I$ using the polynomial Eq. (4) with the coefficients $y_0$, $y_1$, and $y_2$ determined by the least-squares fit of this polynomial to the observed $v_D(z)$.

The dependences of the chord length on other parameters are more subtle and can only be evidenced once the very strong correlation with the line intensity has been taken out. All the regression coefficients for all four stars are listed in Table 2. The first row of numbers for each star gives the $x_i$ values, while the second row of numbers (in brackets) gives $\sigma(x_i)$. Since $x_i/\sigma(x_i)$ is generally larger than unity, we expect $v_D$ to depend in a significant manner on $\chi_e$, $\lambda_0$, and (except for HR 509) $X_m$. An interpretation of these regression coefficients in terms of magnetic fields will be given in Sect. 5. The dependences are illustrated in the other panels of Fig. 2. In Fig. 2b, the relative departures from the fit (4), $(v_D - v_0)/v_D$, are plotted vs. the excitation potential of the lower level. Although the scatter is large, a linear relation between $(v_D - v_0)/v_D$ and $\chi_e$ can be perceived. This relation is emphasized in the figure by the dashed line, whose slope is obtained from a least-squares fit. In Fig. 2c, the magnetic part of the line width, $v_m$, is plotted vs. the magnetic broadening parameter $X_m$. $v_m$ is computed by subtracting from $v_D(0.5)$ all the contributions that are not due to the magnetic field, using the regression coefficients $x_0, \ldots, x_4$ derived through a least-squares fit of the observed $v_D(0.5)$ by Eq. (2):

$$v_m = v_D(z) - x_0 - x_1 S_I - x_2 S_I^2 - x_3 \chi_e v_0 - x_4 \lambda_0^2/v_0. \quad (5)$$

A clear correlation between $v_m$ and $X_m$ is seen; the linear fit corresponding to the regression coefficient $x_5$ is drawn. Note also that it appears from Fig. 2c that the slope of the regression line is to a large extent dictated by the few lines having very large values of $X_m$. If these lines were not included in the analysis, the slope of the regression line would be significantly increased, and the scattered points more uniformly distributed about it. This is illustrated in Fig. 2d, which was obtained by excluding from the regression analysis the two lines with the largest values of $X_m$. Possible reasons for a departure of lines with large $X_m$ from a linear relation between $v_m$ and $X_m$ will be examined below and in Sect. 5.

A possible test to see whether any residual dependence on $S_I$ is present in $(kc\lambda_0)^2 X_m/v_0$ or in $v_m$ is to plot these quantities against $S_I$ and search for possible correlations. Also, if the behaviour of the two anomalous lines has to do with a correlation of this type, it should be visible from such a diagram. As an illustration $(kc\lambda_0)^2 X_m/v_0$ vs. $S_I$ for data from HR 1084 is plotted in Fig. 3a, while $v_m$ vs. $S_I$ for the same data is plotted in Fig. 3b. No correlation is apparent in either of the figures. The two anomalous lines are marked by circled crosses. Crosstalk between line intensity and Zeeman splitting does not appear to be responsible for their anomalous behaviour.

The 42 unblended Fe I lines used in the regression for HR 1084 are tabulated in Table 3, along with their atomic ($\chi_e$, $X_m$), directly measured ($S_I$, $v_D(z=0.5)$) and derived ($v_m(z=0.5)$) parameters. The data provided in this table are sufficient to carry out the rest of the analysis for this star and obtain information on its magnetic field.

## 4. Tests of the validity of the regression equation using solar data

In addition to the illustrative examples and tests based on stellar data discussed in Sects. 3 and 5, we have also carried out some tests to check how valid and unique the regression Eq. (2) is and how reliable its results are using solar data. These tests and their outcome are the subject of the present section.

There are some advantages in performing the tests that are reported hereafter using solar data rather than the stellar spectra that are the object of this study:

(i) The solar data have higher spectral resolution and $S/N$ ratio than the stellar data, so that the presence of small effects can be evidenced or rejected more confidently on the basis of the former.

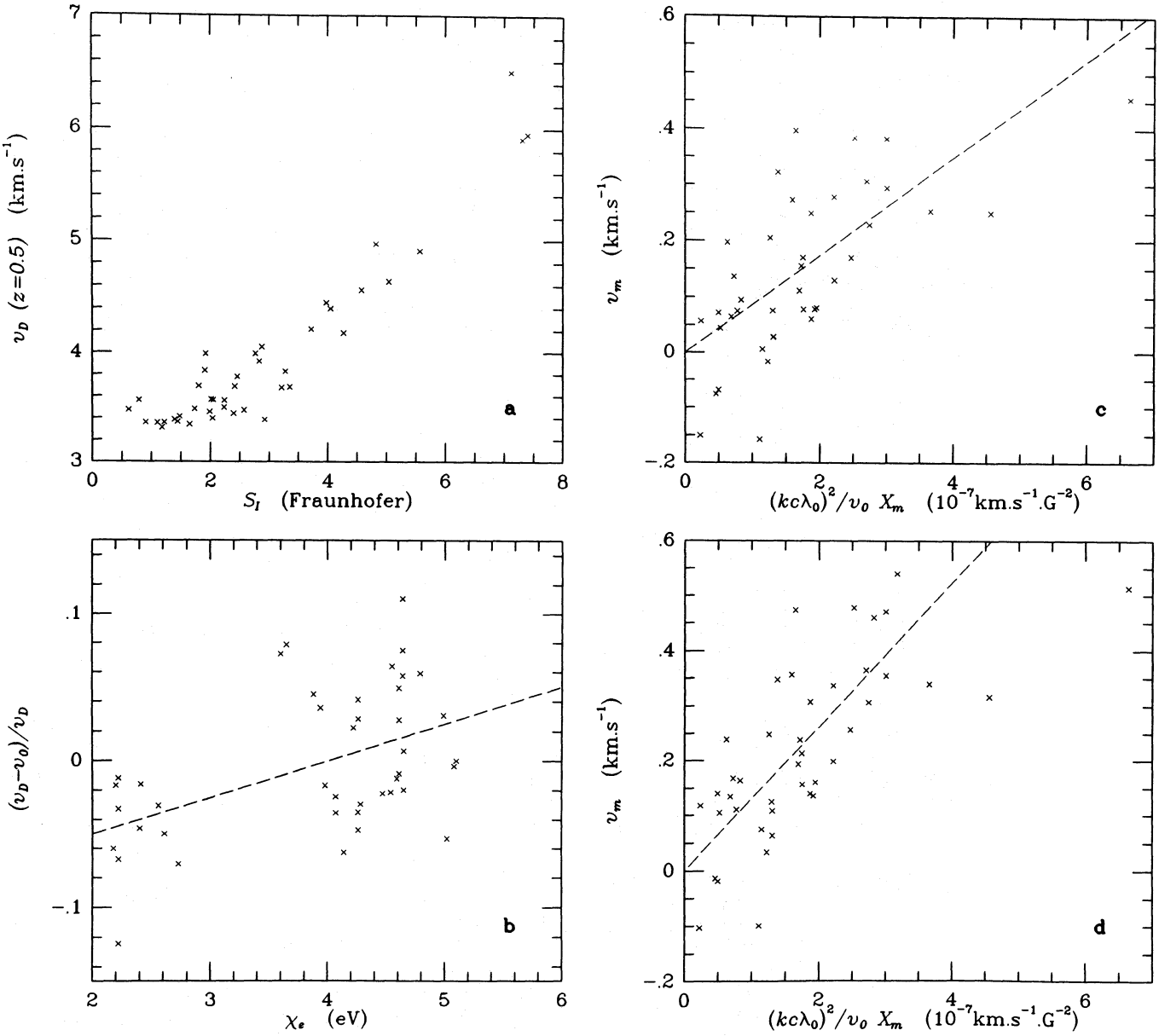


**Fig. 2a–d.** Various dependences of the chord length at half-depth in the line, $v_D$ ($z = 0.5$), are illustrated here: on the line intensity (**a**), on the excitation potential of the lower level of the transition (**b**), and on the magnetic broadening parameter $X_m$ (**c** and **d**; for more details see text). The plots correspond to the star HR 1084

**Table 2.** Regression coefficients

| HR | $x_0$ | | $x_1$ | $x_2$ | $x_3$ | $x_4$ | $x_5$ |
|---|---|---|---|---|---|---|---|
| 509 | 2.06 | | $1.37\ 10^{-1}$ | $3.53\ 10^{-2}$ | $4.44\ 10^{-2}$ | $2.15\ 10^{-8}$ | $0.77\ 10^{-9}$ |
| | (0.14 | ) | ($0.37\ 10^{-1}$) | ($0.66\ 10^{-2}$) | ($0.49\ 10^{-2}$) | ($0.81\ 10^{-8}$) | ($1.90\ 10^{-9}$) |
| 1084 | 1.94 | | $1.00\ 10^{-1}$ | $4.42\ 10^{-2}$ | $4.99\ 10^{-2}$ | $3.14\ 10^{-8}$ | $1.71\ 10^{-8}$ |
| | (0.21 | ) | ($0.44\ 10^{-1}$) | ($0.54\ 10^{-2}$) | ($0.59\ 10^{-2}$) | ($1.31\ 10^{-8}$) | ($0.33\ 10^{-8}$) |
| 1325 | 1.94 | | $7.32\ 10^{-2}$ | $4.91\ 10^{-2}$ | $4.48\ 10^{-2}$ | $2.47\ 10^{-8}$ | $5.85\ 10^{-9}$ |
| | (0.24 | ) | ($5.60\ 10^{-2}$) | ($0.86\ 10^{-2}$) | ($0.79\ 10^{-2}$) | ($1.30\ 10^{-8}$) | ($3.17\ 10^{-9}$) |
| 8387 | 1.53 | | $1.44\ 10^{-1}$ | $4.26\ 10^{-2}$ | $7.40\ 10^{-2}$ | $3.20\ 10^{-8}$ | $1.73\ 10^{-8}$ |
| | (0.35 | ) | ($0.61\ 10^{-1}$) | ($0.62\ 10^{-2}$) | ($1.00\ 10^{-2}$) | ($2.25\ 10^{-8}$) | ($0.57\ 10^{-8}$) |

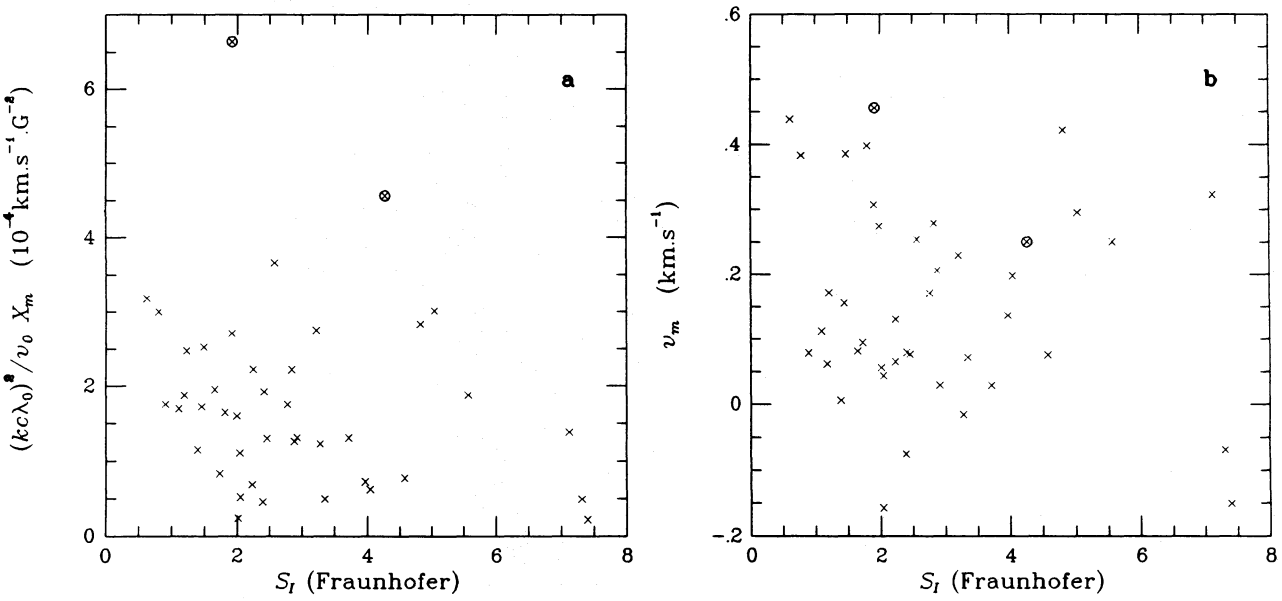


**Fig. 3a and b.** The Zeeman broadening term of the regression $(kc\lambda_0)^2\ X_m/v_0$ (**a**) and the residual line broadening after the removal of all non-magnetic causes, $v_m$ (**b**) vs. line intensity $S_I$, for the star HR 1084. The two lines with the largest expected Zeeman broadening are circled

(ii) Our solar data cover a wider wavelength range and thus contain more lines that can be used for the analysis, so that the statistical significance of the conclusions that are drawn is better than if stellar data were used; furthermore, the availability of a large sample of lines makes it possible to define subsamples in order to perform additional tests.

(iii) For the sun, we have at our disposal both intensity (Stokes I) and circular polarization (Stokes V) recordings; the only contribution to the latter comes from the magnetic parts of the surface, which permits to derive information about the magnetic regions without any contamination from the non-magnetic regions and thus to critically test the analysis performed from the Stokes I spectrum.

It can of course be questioned to which extent the conclusions obtained from tests performed on solar data can be applied to stellar observations. The physical situation in the atmosphere of the considered star can admittedly significantly differ from that in the outer layers of the sun. However,

(i) the same equation satisfactorily represents the behaviour of $v_D$ in the sun and in all the observed stars, and

(ii) the various tests that are reported in the following subsections prove that this equation is very well suited in the solar case and that the addition or the replacement of some terms in it only have negligible effects on the magnetic field diagnosis, even in the much more sensitive solar context.

Consequently, it seems very unlikely that any spurious effect, undetected in the solar case, might significantly alter the conclusions derived about stellar magnetic fields using Eq. (2).

Let us know sketch the guiding lines that have been followed to perform the statistical tests that are reported below. There are two ways in which a line parameter (e.g., line intensity, or wavelength) may affect the value of the coefficient $x_5$ of the magnetic term of Eq. (2). The first is when the general dependence of $v_D$ on $S_I$, $\lambda_0$, or $\chi_e$ is not adequately taken into account. This can be tested by changing individual terms in the regression equation, either by removing them, replacing them by other dependences or by adding additional terms. Second, the magnitude of the Zeeman broadening may itself depend on other parameters, e.g., the way that Zeeman splitting affects the line profile may, to some extent, depend on the saturation of the line, i.e., its intensity, as is suggested by the Milne-Eddington calculations of Stenflo and Lindegren (1977). One way of testing whether such an influence may affect our results is to carry out the regression only for the lines restricted to a relatively narrow range of the parameter under investigation. Since the strongest dependence of $v_D$ is on $S_I$, we shall consider only how $x_5$ depends on $S_I$ of the chosen sample of lines.

Finally, an idea of the reliability of the statistical technique can be obtained by comparing its results with those of other techniques. Since the inter-comparison of stellar magnetic fields derived from the same data by different techniques will be the subject of a separate paper we shall not go into this point in detail here, but only refer to the work of Stenflo and Lindegren (1977), Solanki and Stenflo (1984), Mathys and Stenflo (1986), Schüssler and Solanki (1988), and Brandt and Solanki (1987, and in preparation).

### *4.1. Observational solar data*

We have carried out these tests mostly with solar Stokes I and V spectra obtained near disk centre in active region plages and the quiet network with the McMath telescope of the National Solar Observatory on Kitt Peak and the Fourier transform spectrometer (FTS) polarimeter package. The individual spectra cover approximately 1000–1500 Å, have a spectral resolution of 360000–420000 and a $S/N$ ratio in the continuum of generally 5000–10000. Approximately 150–230 unblended Fe I lines are present per spectrum. Further details are to be found in Stenflo et al. (1984) and Solanki (1987). Each FTS spectrum actually provides us with two individual spectra for testing; firstly the plain intensity (Stokes I) spectrum and secondly the integrated Stokes V spectrum, which is basically an approximation of the Stokes I spectrum produced exclusively in the magnetic features (Solanki and Stenflo, 1984, 1985). An advantage of the integrated Stokes V

**Table 3.** HR 1084 line parameters

| $\lambda_0$ (Å) | $\chi_e$ (eV) | $X_m$ | $S_I$ (F) | $v_D$ (km.s$^{-1}$) | $v_m$ (km.s$^{-1}$) |
|---|---|---|---|---|---|
| 5633.950 | 4.99 | 0.8569 | 3.72 | 4.21 | 0.03 |
| 5635.825 | 4.26 | 0.4000 | 2.23 | 3.50 | 0.06 |
| 5638.268 | 4.22 | 0.5570 | 4.58 | 4.56 | 0.08 |
| 5641.439 | 4.26 | 0.4226 | 4.04 | 4.40 | 0.20 |
| 5646.686 | 4.26 | 1.7168 | 0.62 | 3.47 | 0.44 |
| 5649.988 | 5.10 | 0.1373 | 2.02 | 3.57 | 0.06 |
| 5650.687 | 5.08 | 0.2990 | 2.05 | 3.56 | 0.04 |
| 5651.472 | 4.47 | 1.3553 | 1.22 | 3.36 | 0.17 |
| 5652.319 | 4.26 | 1.0907 | 1.65 | 3.34 | 0.08 |
| 5661.348 | 4.28 | 0.9492 | 1.45 | 3.37 | 0.16 |
| 6065.492 | 2.61 | 0.1929 | 7.40 | 5.95 | −0.15 |
| 6078.498 | 4.79 | 0.4183 | 3.97 | 4.45 | 0.14 |
| 6079.014 | 4.65 | 0.9721 | 2.41 | 3.69 | 0.08 |
| 6082.715 | 2.22 | 1.8679 | 2.57 | 3.47 | 0.25 |
| 6089.572 | 5.02 | 0.5444 | 2.04 | 3.39 | −0.16 |
| 6093.646 | 4.61 | 0.4007 | 1.73 | 3.48 | 0.09 |
| 6094.376 | 4.65 | 0.7973 | 1.10 | 3.35 | 0.11 |
| 6096.668 | 3.98 | 1.1041 | 2.24 | 3.56 | 0.13 |
| 6151.622 | 2.18 | 1.4420 | 3.21 | 3.68 | 0.23 |
| 6157.733 | 4.07 | 0.6480 | 3.28 | 3.83 | −0.02 |
| 6159.380 | 4.61 | 1.3685 | 0.79 | 3.56 | 0.38 |
| 6165.364 | 4.14 | 0.2259 | 2.39 | 3.44 | −0.08 |
| 6173.343 | 2.22 | 2.6345 | 4.27 | 4.18 | 0.25 |
| 6180.208 | 2.73 | 0.2618 | 3.35 | 3.69 | 0.07 |
| 6187.994 | 3.94 | 1.1161 | 2.83 | 3.92 | 0.28 |
| 6213.438 | 2.22 | 1.8660 | 5.04 | 4.64 | 0.29 |
| 6219.289 | 2.20 | 1.2338 | 5.57 | 4.91 | 0.25 |
| 6226.740 | 3.88 | 0.7644 | 1.80 | 3.69 | 0.40 |
| 6232.649 | 3.65 | 1.7002 | 4.82 | 4.97 | 0.42 |
| 6240.651 | 2.22 | 0.6530 | 2.92 | 3.38 | 0.03 |
| 6246.327 | 3.60 | 1.0897 | 7.13 | 6.51 | 0.32 |
| 6252.564 | 2.40 | 0.4011 | 7.32 | 5.91 | −0.07 |
| 6820.373 | 4.64 | 1.0532 | 1.91 | 3.83 | 0.31 |
| 6828.598 | 4.64 | 0.7198 | 2.77 | 3.99 | 0.17 |
| 6837.009 | 4.59 | 0.6514 | 0.90 | 3.36 | 0.08 |
| 6839.834 | 2.56 | 0.6208 | 1.99 | 3.46 | 0.27 |
| 6842.690 | 4.64 | 2.5683 | 1.92 | 3.99 | 0.46 |
| 6843.661 | 4.55 | 0.5197 | 2.88 | 4.05 | 0.21 |
| 6857.248 | 4.07 | 0.6980 | 1.18 | 3.31 | 0.06 |
| 6858.154 | 4.61 | 0.5178 | 2.46 | 3.78 | 0.08 |
| 6861.945 | 2.41 | 0.9492 | 1.48 | 3.42 | 0.38 |
| 6862.496 | 4.54 | 0.4308 | 1.39 | 3.38 | 0.01 |

data is that the filling factor is unity and, therefore, a known quantity.

### 4.2. *Various forms of the regression equation*

In this section we briefly discuss regressions with Eq. (2) amended in one of three ways:

(i) inclusion of an additional term of one of the following forms: $S_I^3$, $S_I^4$, $\lambda_0^4/v_0$, $\lambda_0/v_0$, $\lambda_0^4$, $\lambda_0^2$, $\lambda_0$, $\lambda_0^4 v_0$, $\lambda_0^2 v_0$, $\lambda_0 v_0$, $\lambda_0^4/v_0^2$, $\lambda_0/\sqrt{v_0}$, $\chi_e$, $\chi_e S_I$, $\chi_e/v_0$, $\chi_e^2$, $\chi_e^2/v_0$, $s_e^2 v_0$, $\chi_e^2 v_0^2$, $\chi_e^2 S_I$;

(ii) replacement of one of the terms by one of another form: $S_I \rightarrow S_I^3$, $S_I^2 \rightarrow S_I^3$, $S_I \rightarrow S_I^4$, $S_I^2 \rightarrow S_I^4$, $\lambda_0^2/v_0 \rightarrow \lambda_0^4/v_0$, $\lambda_0^2/v_0 \rightarrow \lambda_0/v_0$, $\lambda_0^2/v_0 \rightarrow \lambda_0^4$, $\lambda_0^2/v_0 \rightarrow \lambda_0^2$, $\lambda_0^2/v_0 \rightarrow \lambda_0$, $\lambda_0^2/v_0 \rightarrow \lambda_0^4 v_0$, $\lambda_0^2/v_0 \rightarrow \lambda_0^2 v_0$, $\lambda_0^2/v_0 \rightarrow \lambda_0 v_0$, $\chi_e v_0 \rightarrow \chi_e S_I$, $\chi_e v_0 \rightarrow \chi_e$, $\chi_e v_0 \rightarrow \chi_e^2 v_0$, $\chi_e v_0 \rightarrow \chi_e^2 v_0^2$;

(iii) removal of one of the terms: $\lambda_0^2/v_0$, $\chi_e v_0$, $S_I$, $S_I^2$.

Although this list is not completely exhaustive, we feel that it is sufficiently comprehensive to illuminate any shortcomings in the regression equation, except in the Zeeman splitting ($x_5$) term itself. We have not tried to empirically change this term, since it was derived from a (simple) model of the Zeeman line broadening, as has been described in detail by Stenflo and Lindegren (1977), and it therefore allows a direct determination of the magnetic parameters. Any purely empirical changes to this term make it lose this important property without giving us additional insight.

After making each change to the regression equation, we have tested how this affects the coefficient of the Zeeman broadening term, $x_5$. The smallest change to $x_5$ was produced by the addition of a further term to Eq. (2). In most of the tested cases the change in $x_5$ was smaller than $0.5\sigma(x_5)$. Somewhat surprisingly the addition of an $S_I^3$ or $S_I^4$ term had only a minuscule effect on $x_5$. This suggests that the regression equation is relatively complete and does take into account all the main dependences of the line width on the various line parameters adequately.

Replacing one term by another often has a somewhat larger influence on $x_5$, but again the change in $x_5$ never exceeded $\sigma(x_5)$ by more than a very small amount, and generally was smaller than $1\sigma$. This suggests that the chosen forms of the individual terms are not critical for the correct determinations of the magnetic field. By far the largest change in $x_5$ was induced when one of the terms of Eq. (2) was left out. The change was of the order of $0.5$–$3\sigma$, depending on the term and on the data. Therefore all the terms already included in Eq. (2) are, more or less, relevant. Note that the smallest change was induced by removing either the $S_I$ or the $S_I^2$ terms.

Finally, we have also tried various forms of Eq. (4) but, like Stenflo and Lindegren (1977), we find that $x_5$ is rather insensitive to the exact form of this equation, as long as it represents the $S_I$ dependence of $v_D$ reasonably well.

We conclude that although we cannot rule out for certain the existence of a more appropriate regression equation, Eq. (2) does seem to be quite adequate for our present purpose, i.e., of deriving the magnetic field parameters of late type stars.

### 4.3. *Regressions of the lines within limited line intensity intervals*

To test whether the $x_5$ coefficient partly absorbs the line intensity dependence of $v_D$ (e.g., due to an inappropriate form of the Zeeman broadening term) only the lines whose intensities $S_I$ lie within a certain interval were used to determine the regression coefficients. The $x_5$ coefficients from a number of such intervals were then compared with each other and with the $x_5$ derived from all the data. Any infiltration of the line intensity dependence of $v_D$ into $x_5$ is expected to show up as a trend in the $x_5$ values obtained from lines of different $S_I$.

Figure 4 shows the $x_5$ values derived from the $z = 0.3$ (squares), $z = 0.5$ (triangles, and $z = 0.7$ (inverted triangles) chords of two solar regions vs. the line intensity. The top row of symbols refers to the $x_5$ values derived from the integrated Stokes V profiles in a quiet network region, the middle row (enlarged filled symbols) to the $x_5$ values derived from the Stokes I spectrum of an active region plage, while the bottom row represents the $x_5$ obtained from the Stokes I data of the quiet network region. The symbols are plotted near the central $S_I$ of the sample of lines used to determine them. Each $S_I$ range has a width of $4F$. Narrower ranges give much the same results, but with error bars which become progressively larger as the ranges get narrower. The error bars correspond to $1\sigma$ confidence limits to $x_5$. Also plotted at the extreme right (around $S_I = 9F$) are the $x_5$ determined from all the unblended Fe I lines in the spectra. In aid of clarity the results for the $I_V$ profiles are plotted only for one region, since both regions have similar $x_5$ values. All the samples, except for the one centred on $6F$, give similar error bars. The lines with intensities in the

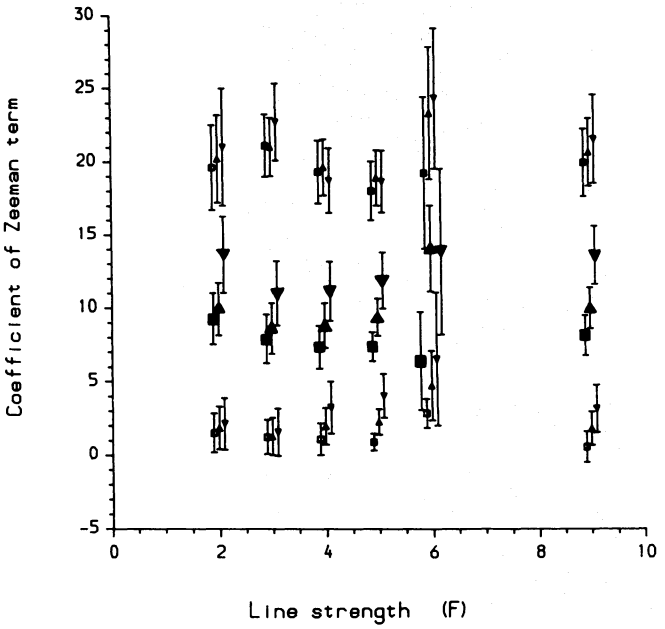


**Fig. 4.** The coefficient $x_5$ of the Zeeman broadening term of the regression equation vs. line intensity. Squares: $x_5$ obtained from the regression of $v_D(z=0.3)$, triangles: $v_D(z=0.5)$, inverted triangles: $v_D(z=0.7)$. Error bars signify $1\sigma$ confidence limits. Top row: integrated Stokes V spectrum data from a solar network region. Middle row (enlarged, filled symbols): Stokes I data from a solar active region. Bottom row: Stokes I data from a solar network region. The $x_5$ plotted near the right edge of the figure (line intensity = 9 F) were derived from the complete data sets, the rest from samples of lines with similar intensities

range 4–8 *F* give more uncertain $x_5$ values due to the rather similar Zeeman splittings of all the lines in this sample.

No particular trend is visible from the figure. The scatter of the $x_5$ values around the mean $x_5$ (derived from the complete sample of lines) is approximately $1\sigma$, as expected if no significant dependence of $x_5$ on $S_I$ exists. However, final certainty regarding this can only be achieved by carrying out radiative transfer test calculations. These are planned for a later paper.

## 5. Interpretation and discussion

The most straightforward interpretation of the regression analysis in terms of a stellar magnetic field will now be presented. For a weak absorption line, at a given point on the stellar surface, it can be shown that the line width $v_D$ in the presence of a weak [1] magnetic field $H$ is approximately related to the line width $v_{D0}$ without a magnetic field through (cf. Stenflo and Lindegren, 1977):

$$v_D \approx v_{D0} + (k^2 c^2 X_m \lambda_0^2 / v_{D0})\, H^2. \tag{6}$$

Actual profiles are averages over the whole visible stellar disk. To deal with them, we assume (as is done by most authors in studies of magnetic fields in late-type stars) that the star's surface can be represented by a two-component model: on the one hand, non-magnetic regions, which are free of any magnetic field, and on the other hand, magnetic regions, in which the magnetic field is supposed to have a single value $H$, the same for all the magnetic regions. Furthermore, we assume (i) that the magnetic regions cover a fraction $\alpha$ of the stellar surface, (ii) that the ratio of the continuum intensity in the magnetic regions to that in the non-magnetic regions is a constant, $\delta_c$, and (iii) that the ratio of the line intensities in the magnetic regions to that in the non-magnetic regions is also a constant, $\delta_l$. $\delta_c$ and $\delta_l$ will differ from unity if the atmosphere in the magnetic regions of the star differs from the atmosphere in the non-magnetic region, as is generally the case on the sun. Then, the local Eq. (6) becomes, for lines integrated over a whole stellar hemisphere:

$$v_D \approx v_{D0} + (k^2 c^2 X_m \lambda_0^2 / v_0)\, \alpha\, \delta_c\, \delta_l\, H^2, \tag{7}$$

so that the $x_5$ coefficient in the regression Eq (2) can readily be interpreted as follows in terms of the magnetic field: $\alpha \delta_c \delta_l H^2 = x_5/(k^2 c^2)$.

Before presenting our results, let us mention here an ambiguity that is present in all the determinations of magnetic fields in late-type stars performed to this date. As can be seen from its definition, the parameter $X_m$ characterizing the sensitivity of the line width to a magnetic field is not a purely atomic parameter, since it depends on the angle $\gamma$ between the magnetic field and the line of sight. In other words, $X_m$ is unambiguously determined only provided that one knows, prior to the analysis, the value of this angle $\gamma$, which is of course not the case. The value of $\gamma$ can in principle be derived through the Stenflo-Lindegren technique by splitting the last term of the regression Eq. (2) into two parts:

$$v_D(z) = x_0 + x_1 S_I + x_2 S_I^2 + x_3 \chi_e v_0 + x_4 \lambda_0^2 / v_0 + x_5' X_m' \lambda_0^2 / v_0 + x_5'' X_m'' \lambda_0^2 / v_0, \tag{8}$$

with $X_m' = 0.5(\bar{g}^2 + X_\sigma + X_\pi)$ and $X_m'' = 0.5(\bar{g}^2 + X_\sigma - X_\pi)$. The regression coefficients $x_5'$ and $x_5''$ are then interpreted as $x_5' = k^2 c^2 \alpha \delta_c \delta_l H^2$ and $x_5'' = k^2 c^2 \alpha \delta_c \delta_l H^2 \langle \cos^2 \gamma \rangle$, where $\langle \cos^2 \gamma \rangle$ is a (suitably weighted) average of $\cos^2 \gamma$ over the stellar disk. In practice, however, our data were found to be insufficiently constraining to settle the value of $\langle \cos^2 \gamma \rangle$, so that this approach could not be applied. Rather, we adhered to the position of previous authors, adopting an a priori chosen average value $\langle \gamma \rangle$. Following Marcy (1984), we used $\langle \gamma \rangle = 34°$ for all the results reported here. Later in this paper we will briefly discuss the implications of this arbitrary (though apparently reasonable) choice.

The values of $fH \equiv \sqrt{\alpha \delta_c \delta_l}\, H$ that we derive from our observations are presented in Table 4. The first two columns give the star's identification, and the third one the number of Fe I lines used for the analysis. In the fourth column we list the values of $fH$; the quoted uncertainty corresponds to $1\sigma$. The last two columns contain separate values of $f^2$ and $H$, deduced as explained below. The results of Table 4 are slightly different from those previously reported elsewhere (Mathys and Solanki, 1988; Solanki and Mathys, 1988). This results from a (hopefully) improved reduction of the observations (evaluating the dark current as described in

**Table 4.** Derived magnetic field values

| Name | HR | No. of lines | $fB$ (G) | $f^2$ | $H$ (G) |
|---|---|---|---|---|---|
| $\tau$ Cet | 509 | 57 | $200 \pm 250$ | | |
| $\epsilon$ Eri | 1084 | 42 | $935 \pm 90$ | 0.10–0.20 | 2090–2960 |
| 40 Eri A | 1325 | 42 | $545 \pm 150$ | $\gtrsim 0.15$ | $\lesssim 1410$ |
| $\epsilon$ Ind | 8387 | 43 | $940 \pm 155$ | 0.08–0.25 | 1880–3320 |

[1] By a weak field we mean that the Zeeman splitting is small compared to the line width.

Sect. 2 rather than from dark exposures). Furthermore, the spectra in the former papers had been measured by S. K. Solanki, those here by G. Mathys, using different codes to compute the line profile parameters. In view of the minute effects looked for, it is not surprising that the slightest differences in the measurements can to some extent affect the deduced results. Nevertheless, the present results are quite consistent with those that we have previously published, except for some small discrepancies in the evaluated uncertainties, whose source still has to be found, but which do not question the overall validity of our magnetic field diagnosis.

From Table 4, it can be seen that we definitely detect a magnetic field in HR 1084 and HR 8387 as well as, most probably, in HR 1325. On the other hand, our analysis of HR 509 reveals no significant field. Independent field detections in HR 1084 and HR 1325 have been reported by several authors (e.g. Marcy, 1984; Gray, 1984; Saar, 1988); all these authors except Gray also failed to detect any magnetic field in HR 509. We have found no published measurement of the magnetic field of HR 8387.

As mentioned in Sect. 3, it can be seen from Fig. 2c that the lines with large values of $X_m$, in particular the two lines $\lambda\lambda$ 6173.34 and 6842.69 [2], deviate appreciably from the linear relation between $X_m$ and $v_m$ defined by the other lines of the sample. The effect is observed not only in HR 1084, which is the case represented in Fig. 3, but also in HR 1325 and HR 8387. This indicates that the deviation is very likely not the result of random measurement errors. Although we cannot rule out the possibility that these two lines are affected by blends, we feel that at least part of the deviation is due to the intrinsic properties of the considered lines and thus has to be understood.

A possible source of deviation is an inadequate choice of the average angle $\langle\gamma\rangle$ between the magnetic field and the line of sight. To test it, we have repeated the analysis of HR 1084 for various values of $\langle\cos^2\gamma\rangle$, between 0 and 1. The effect on the derived value of $fH$ is illustrated in Fig. 5, where it is seen to be quite significant. Note that the ratio $fH/\sigma(fH)$ hardly changes with the value of $\langle\gamma\rangle$ (it decreases very slightly, monotonically, from $\langle\gamma\rangle = 0°$ to $\langle\gamma\rangle = 90°$). Otherwise, as could have been expected from the expression of $X_m$, the agreement of $\lambda\lambda$ 6173.34 and 6842.59 with the other lines is improved for larger $\langle\gamma\rangle$. However these two lines keep deviating from the mean trend, even in the unrealistic limit $\langle\gamma\rangle = 90°$, so that the choice of $\langle\gamma\rangle$ does not appear to be responsible for their discrepant behaviour.

On the other hand, it must be recalled that the expression (7) of the magnetic broadening of the line that is used for the present interpretation is valid only in the weak field limit, viz. when the magnetic broadening is small compared to the intrinsic line width. For the lines having the largest values of $X_m$, this may no longer be a good approximation (see Mathys and Stenflo, 1987). This can be tested through numerical simulations. Such simulations will be presented in a subsequent paper. In the meanwhile, we repeated the analysis (see Fig. 2d) omitting the disputed lines, in order to evaluate how they affect the derived values. For the three stars in which we detect a magnetic field, the value of $fH$ is increased, as expected: for HR 1084, we get $fH = (1140 \pm 105)$ G, for HR 1325, $fH = (750 \pm 160)$ G, and for HR 8387, $fH = (1180 \pm 185)$ G. The significant differences between these figures and those in Table 4 show the need for a better understanding of what is actually happening to the large $X_m$ lines. This will be part of our future work.

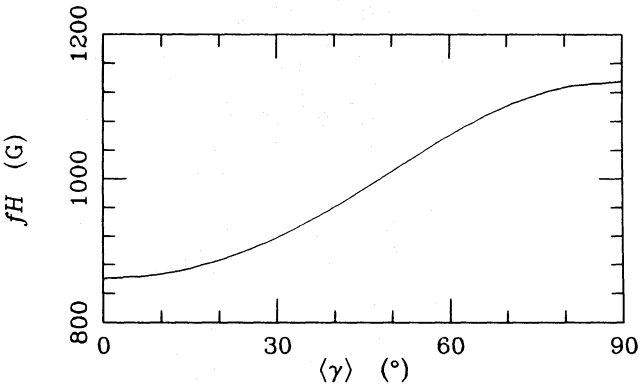


**Fig. 5.** Dependence of the derived value of the product $fH$ on the assumed average value $\langle\gamma\rangle$ of the angle between the magnetic vector and the line of sight, for the star HR 1084

Up to now, we have determined the product $fH$. The Stenflo-Lindegren technique permits us to go further into the diagnosis. On the one hand, for a filling factor $\alpha$ less than 1, the part of a typical weak photospheric line nearer the continuum is more strongly affected by the magnetic field than the line core, so that performing the same regression analysis for the line width at various depths above the line bottom and comparing the results permits in principle to separate $f$ and $H$. The values of $f^2$ and $H$ in Columns 5 and 6 of Table 4 were derived by comparing with observations in solar active regions covering a range of filling factors (Brandt and Solanki, 1987, and in preparation). More reliable values for $f$ and $H$ can be obtained by comparing with profiles calculated using a more sophisticated model involving radiative transfer. However, this is beyond the scope of the present paper.

On the other hand, the Stenflo-Lindegren technique also provides the opportunity of deciding whether the measured magnetic fields issue from hot or cool regions of the stellar surface or, in other words, from stellar plages or spots. These are defined in analogy to the sun, where we can classify magnetic fluxtubes into two main types: those with diameters greater than a few thousand km (sunspots), which are darker and cooler than their surroundings, and those with diameters of generally less than a few hundred km, which are brighter and hotter than their surroundings. Groups of small fluxtubes make up solar plages. As we have pointed out earlier [e.g. Eq. (7)], the magnetic line broadening depends on the relative intensities of the lines in the magnetic and non-magnetic regions. It is well known that a change in temperature will affect the intensities of spectral lines considerably, with the exact influence depending on various properties of the transition, for example the excitation potential of the lower level. We can use the Stenflo-Lindegren technique to obtain information on this important quantity, by sorting the lines of the sample into a low excitation and a high excitation groups, performing the analysis of these two groups separately, and comparing the results. Only for HR 1084 were the statistics good enough to allow this to be performed, and we deduced that the observed field is concentrated in regions that are hotter than the non-magnetic part of the atmosphere. Once again, a detailed modelling of the line formation will have to be performed to get more quantitative results.

[2] Incidentally, these two lines were employed respectively by Marcy (1984) and by Robinson et al. (1980) for their studies of stellar magnetic fields.

Finally, how does our method of magnetic field diagnosis compare with others? The question cannot be fully answered yet. A comparison of results obtained through various techniques can only be carried out using the same observational data, since magnetic fields in late-type stars have been found to undergo significant, apparently irregular, variations, sometimes on short-time scales (a few days). Thus, all that can be said at present is that allowing for the intrinsic variations of the stellar magnetic fields, our results are compatible with those published by other authors for the stars in common. Since our approach is quite distinct from those previously used, it also provides independent confirmation of the magnetic fields measured by other researchers. On the other hand, our technique appears to be superior to those previously used because of its relative unsensitivity to line blends (which increase the scatter about the best fits but should not falsify the conclusions) and of its ability to set constraints on the temperature differences between magnetic and non-magnetic regions of the stellar surface. One of its possible pitfalls, which must be investigated, is the fact that the lines in different wavelength ranges are observed at different times over the night, which may be troublesome if rapid variations occur.

## 6. Conclusion

Using observations obtained with the ESO CES and an original (within the present context) analysis technique, we were able to diagnose magnetic fields in some late-type dwarfs. Though they are still debatable in some respects, the results that we obtain are entirely compatible with previous determinations achieved with other techniques. We wish to stress that the results presented in this paper are preliminary in nature and that future progress will come from a more sophisticated interpretation, involving a more realistic modelling of the line formation, which will permit us to better ascertain the exact values of the magnetic-field-related parameters that are derived. In a next step we intend to model the line formation using a Milne-Eddington atmosphere, i.e., to calculate line profiles using the Unno-Rachkovsky solutions to the transfer equations for spectral lines in a magnetic field (Unno, 1956; Rachkovsky, 1967). This should allow us to study under controlled conditions how Zeeman splitting affects widely different line profiles. In addition, by applying exactly the same regression to the calculated line profiles (after suitably broadening them by the instrumental profile, stellar rotation and turbulence velocity) as the observed lines, it should be possible with the help of a least squares fitting tehnique to derive $f$ and $B$ individually without having to compare with solar data. A comparison of the results obtained with different methods using the same observational data is also foreseen.

## References


Babcock, H.W.: 1947, *Astrophys. J.* **105**, 105

Borra, E.F., Edwards, G., Mayor, M.: 1984, *Astrophys. J.* **284**, 211

Brandt, P.N., Solanki, S.K.: 1987, in *The Role of Fine-Scale Magnetic Fields on the Structure of the Solar Atmosphere*, eds. E.-H. Schröter, M. Vázquez, A.A. Wyller, Cambridge University Press, Cambridge, p. 82

Giampapa, M.S., Golub, L., Worden, S.P.: 1983, *Astrophys. J. Letters* **268**, L 121

Gondoin, Ph., Giampapa, M.S., Bookbinder, J.A.: 1985, *Astrophys. J.* **297**, 710

Gray, D.F.: 1984, *Astrophys. J.* **277**, 640

Landi Degl'Innocenti, E.: 1980, *Solar Phys.* **77**, 285

Marcy, G.W.: 1984, *Astrophys. J.* **276**, 286

Mathys, G., Solanki, S.K.: 1988, in *The Impact of Very High S/N Spectroscopy on Stellar Physics*, *IAU Symp.* **132**, eds. G. Cayrel de Strobel, M. Spite, Kluwer, Dordrecht, p. 325

Mathys, G., Stenflo, J.O.: 1986, *Astron. Astrophys.* **168**, 184

Mathys, G., Stenflo, J.O.: 1987, *Astron. Astrophys. Suppl.* **67**, 557

Rachkovsky, D.N.: 1967, *Izv. Krymsk. Astrofiz. Obs.* **37**, 56

Robinson, R.D.: 1980, *Astrophys. J.* **239**, 961

Robinson, R.D., Worden, S.P., Harvey, J.W.: 1980, *Astrophys. J. Letters* **236**, L 155

Saar, S.H.: 1988, *Astrophys. J.* **324**, 441

Saar, S.H., Linsky, J.L.: 1985, *Astrophys. J. Letters* **299**, L 47

Saar, S.H., Linsky, J.L., Beckers, J.M.: 1986, *Astrophys. J.* **302**, 777

Schüssler, M., Solanki, S.K.: 1988, *Astron. Astrophys.* **192**, 338

Solanki, S.K.: 1987, Ph.D. Thesis, E.T.H., Zürich

Solanki, S.K., Mathys, G.: 1988, in *Activity in Cool Star Envelopes*, eds. O. Havnes et al., Reidel, Dordrecht, p. 39

Solanki, S.K., Stenflo, J.O.: 1984, *Astron. Astrophys.* **140**, 185

Solanki, S.K., Stenflo, J.O.: 1985, *Astron. Astrophys.* **148**, 123

Stenflo, J.O., Harvey, J.W., Brault, J.W., Solanki, S.K.: 1984, *Astron. Astrophys.* **131**, 33

Stenflo, J.O., Lindegren, L.: 1977, *Astron. Astrophys.* **59**, 367

Sugar, J., Corliss, C.: 1985, *Atomic Energy Levels of the Iron-Period Elements: Potassium through Nickel*, J. Phys. Chem. Ref. Data **14**, Suppl. 2

Unno, W.: 1956, *Publ. Astron. Soc. Japan* **8**, 108